PHYSICAL REVIEW B VOLUME 12, NUMBER 5 1 SEPTEMBER 1975

Magnetic phase transitions in anisotropic Heisenberg antiferromagnets. I. $MnCl_2 \cdot 4H_2O$†

J. E. Rives and V. Benedict*
Department of Physics and Astronomy, University of Georgia Athens, Georgia 30602
(Received 29 January 1975)

Differential magnetic susceptibility measurements have been used to study the magnetic phase transitions in antiferromagnetic $MnCl_2 \cdot 4H_2O$ between 0.3 and 1.6 K. The antiferromagnetic to spin-flop (SF) transition is shown to be a first-order phase transition below 0.4 K. The SF to paramagnetic transition is observed to have a predominantly $T^{5/2}$ temperature dependence, while spin-wave theory predicts a $T^{3/2}$ dependence. From the values of the critical fields, extrapolated to $T = 0$, the exchange and anisotropy constants are determined. The results are consistent with a Heisenberg model of isotropic exchange with a biaxial single-ion-type anisotropy.

I. INTRODUCTION

The behavior of antiferromagnetic materials in magnetic fields depends strongly on the relative magnitudes of the exchange and anisotropy energies. For example, if the anisotropy energy is somewhat less than the exchange energy a simple two-sublattice antiferromagnet can have three distinct phases, antiferromagnetic (AF), spin-flop (SF), and paramagnetic (P). $MnCl_2 \cdot 4H_2O$ ($T_N = 1.62$ K) exhibits simple antiferromagnetic order with moderately small anisotropy and is a good example of such a system.

The phase transitions in $MnCl_2 \cdot 4H_2O$ have been previously studied using a variety of techniques.[1-7] In most of these studies the fields that were used were relatively small so that only the AF-to-SF and the AF-to-P phase boundaries were accessible. The studies of Rives,[1] Giauque *et al.*,[2] and Reichert and Giauque[3] were more complete. Rives used differential magnetic susceptibility measurements to map out the H-T phase diagram in the preferred direction. Giauque *et al.* measured the specific heat and magnetization and made adiabatic measurements with the external field alternately along the crystallographic c axis, b axis, and perpendicular to the bc plane.

The crystal structure and positional parameters of most of the atoms in $MnCl_2 \cdot 4H_2O$ were determined by x-ray diffraction by Zalkin *et al.*[8] A refinement of the hydrogen positions was determined by neutron diffraction by El Saffar and Brown.[9] The magnetic structure was studied using NMR techniques by Spence and Nagarajan,[10] and more recently, fully determined by neutron diffraction by Altman *et al.*[11] The crystal belongs to the monoclinic system with the angle $\beta = 99.74°$.

There has been disagreement in the literature concerning the preferred direction for spin alignment in this compound. The c axis and the direction perpendicular to the ab plane (c' direction) have been claimed to be the proper preferred direction. The neutron-diffraction measurements of Altman *et al.*[11] indicate that the preferred direction is in the c'-c plane 2.8° from the c' direction, or 7° from the crystallographic c axis. Experiments that were carried out with the external field along the c axis were, therefore, performed with the field displaced as much as 7° from the preferred direction. This is of particular importance at the AF-to-SF transition. It is well known that this transition should be first order, because of the finite increase in magnetization in going from the AF state to the SF state. However, Rohrer and Thomas[12] and Blazey *et al.*[13] have recently reported a mean-field calculation which demonstrates that the first-order behavior will be observed only if the external magnetic field is oriented within a small critical angle relative to the preferred direction. The full significance of this point as it relates to $MnCl_2 \cdot 4H_2O$ will be discussed in Sec. IV.

We wish to report our measurements of the differential magnetic susceptibility on spherical samples of $MnCl_2 \cdot 4H_2O$ between 0.3 and 1.6 K. Special care was taken to ensure that the external field was aligned along the experimentally determined preferred direction. Measurements were also made with the field along each of the two perpendicular directions (a and b axes). The magnetic phase boundaries are determined from these measurements.

Particular care was taken in the determination of the behavior near the AF-to-SF transition. We shall show in Sec. IV that it is indeed possible to observe first-order behavior at this phase boundary if the field is properly aligned and if the magnetic properties of the system are expressed in terms of the proper shape-independent internal field.

We shall also show that serious discrepancies exist between the observed temperature dependence of the phase boundaries that border the paramagnetic state at low temperatures and the temperature behavior expected from spin-wave theory for a simple-cubic model.

II. THEORY

The case of a simple two-sublattice antiferromagnet in an external field has been treated extensively by a variety of techniques. Nagamiya, Yosida, and Kubo[14] reviewed the molecular-field approach and the early statistical theories. The phase transitions in an orthorhombic crystal were studied by Gorter and Van Peski-Tinbergen[15] using a mean-field approach. The AF-to-SF and the P-to-SF phase transitions were studied by Anderson and Callen[16] by a Green's-function analysis of the Heisenberg antiferromagnet with uniaxial anisotropy. The temperature dependence of the phase boundaries at low temperatures was determined by treating spin-wave interactions in a manner similar to that of Dyson[17] in the ferromagnetic case. Using spin-wave theory, including spin-wave interactions, Feder and Pytte[18] determined the temperature dependence of the phase boundaries for a Heisenberg antiferromagnet with both uniaxial single-ion anisotropy and anisotropic exchange. Wang and Callen[19] studied the limits of stability of the SF phase in both the low- and high-field limits to determine the conditions for the SF-to-AF and the SF-to-P phase transitions.

A. Spin-wave theory

The Hamiltonian studied by Feder and Pytte[18] which includes intersublattice interactions only can be written in the form

$$\mathcal{H}=2J\sum_{\langle i,j\rangle}\vec{S}_i\cdot\vec{S}_j+K\sum_{\langle i,j\rangle}S_{iz}S_{jz}-L\left(\sum_i S_{iz}^2+\sum_j S_{jz}^2\right)-\mu H\left(\sum_i S_{iz}+\sum_j S_{jz}\right), \tag{1}$$

where the sum $\langle i,j\rangle$ is taken over all nearest-neighbor pairs, and i and j refer to the two sublattices. The terms, in order, represent the isotropic exchange, anisotropic exchange, uniaxial anisotropy, and Zeeman energies with J, K, and L the exchange and anisotropy constants for the appropriate terms. The z axis is taken as the preferred direction, and H is applied along the z axis.

The field-dependent spin-wave dispersion relations are determined from solutions to Eq. (1). The phase transitions occur at those fields which yield zero-energy spin-wave modes. In the case of uniaxial anisotropy hysteresis is predicted at the first-order AF-to-SF phase boundary.[16,18,19] Specifically, the limit of stability of the AF phase for increasing fields h_{sf}^{+} exceeds the limit of stability of the SF phase for decreasing fields h_{sf}^{-}. No hysteresis is predicted in the case of anisotropic exchange.[18]

Experimentally, in a quasistatic experiment it is the true thermodynamic critical field $H_{\parallel}^{sf}$ which is normally observed, since there are fluctuations present of sufficient energy to prevent the system from "superheating." Since spin-wave theory predicts only the limits of stability, it is of interest to compare h_{sf}^{+}, h_{sf}^{-}, and $H_{\parallel}^{sf}$ in the case of uniaxial anisotropy. Using the experimentally determined values of the exchange and anisotropy energies given in Sec. IV for $MnCl_2\cdot 4H_2O$, we find to first order in the spin-wave corrections,

$$h_{sf}^{+}:H_{\parallel}^{sf}:h_{sf}^{-}=1.001:1:0.832\ .$$

There is a 17% difference in the two limits of stability; however, the limit of stability of the AF phase differs from the true thermodynamic critical field by only 0.1%. Thus for practical purposes we can substitute $H_{\parallel}^{sf}$ for h_{sf}^{+} in the foregoing discussions.

At $T=0$ the critical fields can readily be expressed in terms of the effective exchange field h_E and the effective anisotropy field h_A for both types of anisotropy. At the AF-to-SF phase boundary we have

$$H_{\parallel}^{sf}(0)=(2h_Eh_A+h_A^2)^{1/2}\ , \tag{2}$$

where $h_E=2SzJ/\mu$, $h_A=2S\xi^2L/\mu$ for uniaxial anisotropy, $h_A=SzK/\mu$ for anisotropic exchange, and $\xi^2=1-1/2S$. The SF-to-P critical field for uniaxial anisotropy can be written

$$H_{\parallel}^{c}(0)=2h_E-h_A\ , \tag{3}$$

whereas for anisotropic exchange we get

$$H_{\parallel}^{c}(0)=2h_E+h_A\ . \tag{4}$$

The temperature dependence of each of the phase boundaries is determined by including spin-wave interactions in the treatment. For the AF-to-SF phase boundary Feder and Pytte[18] find, for $k_BT/g\times\mu_BH_{\parallel}^{sf}(0)\ll 1$,

$$H_{\parallel}^{sf}(T)/H_{\parallel}^{sf}(0)=1-AT^{3/2}+BT^{5/2}\ , \tag{5}$$

where $H_{\parallel}^{sf}(0)$ in this relation contains a small temperature-independent spin-wave correction to Eq. (2). For uniaxial anisotropy

$$A=(4z^{3/2}/\pi^2)\tilde{L}^2(1+\tilde{L})\,\Gamma(\tfrac{3}{2})\,\zeta(\tfrac{3}{2})\times S^{-1}[k_B/g\mu_BH_{\parallel}^{sf}(0)]^{3/2}$$

and

$$B=(2z^{3/2}/\pi^2)\tilde{L}\,\Gamma(\tfrac{5}{2})\,\zeta(\tfrac{5}{2})\times S^{-1}[k_B/g\mu_BH_{\parallel}^{sf}(0)]^{5/2}\ .$$

For anisotropic exchange $A=0$ and

$$B=(z^{3/2}/2\pi^2)\tilde{K}(1+\tilde{K})(1+\tilde{K}/2)S^{-1}\,\Gamma(\tfrac{5}{2})\,\zeta(\tfrac{5}{2})\times[k_B/g\mu_BH_{\parallel}^{sf}(0)]^{5/2}\ .$$

In the above relations $\zeta(x)$ is the Riemann zeta function, $\Gamma(x)$ is the gamma function, z is the num-

ber of nearest neighbors, S is the spin quantum number, $\tilde{L}$ is the reduced anisotropy constant $L/2zJ$, and $\tilde{K}$ is the reduced anisotropy constant $K/2J$.

The temperature dependence of the SF-to-P phase boundary is of particular importance since, according to Anderson and Callen, [16] it is directly related to the temperature dependence of the renormalized spin-wave energies. For a simple-cubic model with uniaxial anisotropy Anderson and Callen find

$$H_{\parallel}^{c}(T)/H_{\parallel}^{c}(0) = 1 - C_1 T^{3/2} - C_2 T^{5/2} , \tag{6}$$

where

$$C_1 = 2\zeta(\tfrac{3}{2})(3/2\pi)^{3/2} S^{-1}(k_B/g\mu_B h_E)^{3/2}$$

and

$$C_2 = [3h_E/2H_{\parallel}^{c}(0)]\,\zeta(\tfrac{5}{2})(3/2\pi)^{3/2} S^{-1}(k_B/g\mu_B h_E)^{5/2} .$$

Feder and Pytte[18] calculate only the $T^{3/2}$ term, which is valid for both types of anisotropy with a coefficient of the same magnitude as C_1 above.

With the magnetic field applied along a direction perpendicular to the preferred direction, there is only a single transition from the AF state to the P state. Keefer[20] discusses this case for biaxial anisotropy in a first-order spin-wave theory. In this treatment the zero-wave-vector spin-wave mode goes to zero energy at $H = 2h_E$. This result appears not to take proper account of the anisotropy and, thus, it is necessary to look to mean-field theory to extend our treatment to perpendicular directions.

B. Mean-field theory

In a mean-field treatment the anisotropy can be introduced in a phenomenological way in terms of the anisotropy energy given by[14,21]

$$E_A = -K(\gamma_+^2 + \gamma_-^2)/2 , \tag{7}$$

where γ is the direction cosine of the magnetization, the subscripts refer to the two sublattices, and K is the anisotropy constant. This leads to the definition of an effective anisotropy field h_A which takes on the maximum value K/M_0, where M_0 is the saturated value of the sublattice moment.

At $T = 0$, with this definition of h_A and an appropriate definition of h_E which relates the molecular-field constant to the exchange constant, [21] one obtains for $H_{\parallel}^{sf}(0)$ and $H_{\parallel}^{c}(0)$ expressions identical to Eqs. (2) and (3). With the applied field perpendicular to the preferred direction the critical field for the single AF-to-P transition $H_{\perp}^{c}(0)$ is found to be

$$H_{\perp}^{c}(0) = 2h_E + h_A . \tag{8}$$

Equations (3) and (8) provide a unique determination of h_E and h_A from the experimentally determined critical fields for the case of uniaxial anisotropy.

In the case of anisotropic exchange one obtains[13]

$$H_{\parallel}^{c}(0) = H_{\perp}^{c}(0) = 2h_E + h_A ; \tag{9}$$

therefore an experimental determination of the two critical fields $H_{\parallel}^{c}(0)$ and $H_{\perp}^{c}(0)$ makes it possible to distinguish between the two types of anisotropy if one is dominant in a given system.

If the two perpendicular directions are not equivalent, a uniaxial model is insufficient. For this case a biaxial, or orthorhombic, anisotropy model has been investigated. [14,21] There are two distinct anisotropy fields h_{A1} and h_{A2} which are related to two anisotropy constants K_1 and K_2 in the same way as in the uniaxial case. With the applied field along the preferred direction, the critical fields $H_{\parallel}^{sf}(0)$ and $H_{\parallel}^{c}(0)$ are again identical to the spin-wave results in Eqs. (2) and (3), but with h_{A1} substituted for h_A. For the perpendicular directions Eq. (8) must be replaced by two relations,

$$H_{\perp 1}^{c}(0) = 2h_E + h_{A1} \tag{10}$$

and

$$H_{\perp 2}^{c}(0) = 2h_E + h_{A2} . \tag{11}$$

A measurement of the three critical fields bordering the paramagnetic state, thus, is sufficient for the determination of h_E, h_{A1}, and h_{A2}.

The AF-to-SF transition has been studied in more detail recently by Rohrer and Thomas[12] and Blazey *et al.*[13] within the mean-field approximation. They investigated the limits of stability of the magnetic phases as a function of both magnetic strength and direction. They find that the AF-to-SF transition is first order only if the applied field is aligned within a certain critical angle ψ_c relative to the preferred direction. A good approximation for ψ_c at $T = 0$ for uniaxial anisotropy is given by $\psi_c \simeq h_A/2h_E$. This is an extremely restrictive condition for a large number of antiferromagnetic compounds which have a relatively small anisotropy energy. In materials such as $MnCl_2 \cdot 4H_2O$ we expect ψ_c to be of the order of several degrees, which should make it possible to observe the true first-order nature of the transition.

III. EXPERIMENTAL PROCEDURE

A. Sample preparation

The single crystals of $MnCl_2 \cdot 4H_2O$ used in this work were grown by evaporation from saturated solution at room temperature. Spherically shaped samples of approximately 1-cm^3 volume were fashioned from large single crystals. After shaping, the samples were dried for a short time in a desiccator, removed, and coated immediately with GE 7031 varnish for protection against dehydration.

Treated in this manner, the samples lasted indefinitely, even after many temperature cycles to liquid-helium temperatures.

B. Temperature measurements

Speer nominally 470-Ω, $\frac{1}{2}$-W carbon resistors were used as secondary thermometers throughout the entire temperature range of the experiments. They were calibrated against the 1958 ^{4}He vapor-pressure scale in the range 1.5 to 4.2 K, and against the 1962 ^{3}He vapor-pressure scale from 0.6 to 1.8 K. Below 0.6 K the resistors were calibrated against the susceptibility of cerium magnesium nitrate. The resistance was least-squares fitted to the relation

$$\frac{1}{T}=\sum_{n=-1}^{4} A_n(\ln R)^n \tag{12}$$

to an absolute accuracy of ± 2 mK, except near 1.0 K, where the accuracy was no better than ± 5 mK.

The thermometers were mounted in good thermal contact with a liquid-^{3}He refrigerator, which was situated some 15 cm outside the windings of a superconducting solenoid. With this placement magnetoresistance corrections for the thermometer were negligible. The thermal relaxation time between the thermometer and the sample was about 1 sec, but since data were always taken only after the temperature and field had been stabilized for more than 1 min, no appreciable error was introduced by this arrangement of the thermometer.

C. Susceptibility measurements

The spherical sample was rigidly mounted in a brass goniometer in good thermal contact with the ^{3}He refrigerator and positioned in the center of a superconducting solenoid. The goniometer could be rotated about two mutually perpendicular axes to allow accurate alignment of the crystal relative to the direction of the external field. Compensated mutual-inductance coils were positioned symmetrically within the bore of the superconducting solenoid with the sample in the center of one-half of the secondary coil. The mutual inductance is proportional to the susceptibility of the sample; however, absolute values of the susceptibility are obtained only after calibration of the entire system. The mutual inductance was measured with a Crytronics mutual-inductance bridge, which has a resolution of $\simeq 8\times10^{-4}$ H. The bridge was calibrated by measuring a series of precision mutual inductors over the entire range of the bridge. The details of the calibration of the coil system are described below. Over all, the system was capable of measuring changes in the susceptibility of the order of 0.1×10^{-6} emu/cm^3 in zero field, and owing to the effect of the superconducting solenoid 1.0 $\times10^{-6}$ emu/cm^3 with the solenoid energized. However, owing to uncertainties in the calibration procedure discussed below, there is an over-all uncertainty of 1.5% in the absolute value of the susceptibility. The ac measuring field was $\simeq 0.30$ Oe throughout the experiment.

D. Calibration of mutual-inductance coil system

The mutual-inductance method that is used in these experiments measures the susceptibility in arbitrary units; therefore, it was necessary to calibrate these measurements to obtain absolute susceptibility values. Gijsman, Poulis, and Van den Handel[7] measured the magnetization of $MnCl_2\cdot 4H_2O$ along the crystallographic c axis down to 1.2 K, and Reichert and Giauque[3] extended these measurements down to 0.4 K. The differential susceptibility along the c axis can be calculated from those results. However, the neutron-diffraction measurements of Altman *et al.*[11] indicate that the preferred direction differs from the c axis by 7°. The data along the c axis must be corrected to give the susceptibility along the preferred direction.

From mean-field theory we have

$$\chi_\theta=\chi_\parallel\cos^2\theta+\chi_\perp\sin^2\theta\ ,$$

and thus

$$\frac{\chi_\parallel}{\chi_\theta}=\frac{1-(\chi_\perp/\chi_\theta)\sin^2\theta}{\cos^2\theta}\ . \tag{13}$$

In the case of $MnCl_2\cdot 4H_2O$ the angle $\theta=7°$. Below $T=1.0$ K the perpendicular susceptibility has not been determined; however, the susceptibility in the spin-flop state $\chi_\parallel^{sf}$ has been measured by Reichert and Giauque.[3] Again from mean-field theory we have[21]

$$\chi_\perp=\frac{1}{A+K_1/2M_0}\ , \tag{14}$$

while

$$\chi_\parallel^{sf}=\frac{1}{A-K_1/2M_0}\ , \tag{15}$$

where M_0 is the sublattice moment at $T=0$, A is the molecular-field constant, and K_1 is either the uniaxial anisotropy constant, or the smaller of the two biaxial anisotropy constants. From Eqs. (3) and (8) the ratio of the two susceptibilities at $T=0$ is

$$\chi_\perp/\chi_\parallel^{sf}=H_\parallel^c(0)/H_{\perp 1}^c(0)\ ,$$

which from the experimentally determined critical fields (see Sec. IV) gives a ratio of 0.81.

As an example of the magnitude of the angular correction of the data, at $T=0.4$ K from Reichert and Giauque[3] we find $\chi_\parallel^{sf}=154\times10^{-4}$ emu/cm^3, in good agreement with the value of 160×10^{-4} emu/cm^3

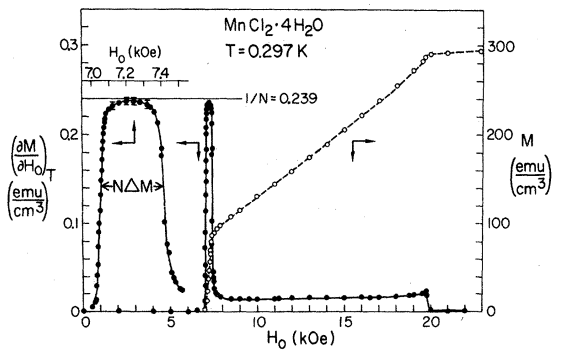

FIG. 1. Differential magnetic susceptibility and magnetization of $MnCl_2 \cdot 4H_2O$ as a function of external field along the preferred direction at 0.297 K. ●, susceptibility (left-hand scale); o, magnetization (right-hand scale).

calculated from Eq. (15). In the limit $H = 0$, $\chi_\theta(\theta = 7°) = 5.8 \times 10^{-4}$ emu/cm^3. From Eq. (13) we obtain $\chi_{II}/\chi_\theta = 0.626$ at $T = 0.4$ K. Using the above angular corrections to obtain a calculated value for χ_{II} at $H = 0$ the calculated relation between the mutual inductance and the susceptibility is given by χ(emu/cm^3) $= 5.46 \times 10^{-4}(M - M_{ref})$ (μH), where M_{ref} is the mutual inductance with the sample removed.

IV. RESULTS AND ANALYSIS

A. Determination of preferred direction of spin alignment

Initially the susceptibility was measured at a series of angles relative to the c' direction in order to determine precisely the preferred direction. The angular dependence of the AF-to-SF transition provides a very accurate test of proper alignment. The large peak in the differential susceptibility, as a function of external field, which accompanies this transition should have a maximum height and minimum width with the field along the preferred direction. In addition, the value of the field at the peak should be a minimum. The orientation of the crystal which optimized all these quantities was taken as the preferred direction. The uncertainty in the preferred direction from these measurements was $\pm 2°$ in the c-c' plane and $\pm 1°$ for out-of-plane rotations. Within this experimental uncertainty, the direction that was determined from these measurements was later found, by neutron diffraction, to agree with the direct determination of Altman *et al.*[11]

B. AF-to-SF transition

Extensive measurements of the susceptibility were made at four different temperatures in order to obtain detailed information about the nature of the AF-to-SF transition. At other temperatures measurements were carried out only in the neighborhood of the transitions in order to determine the temperature dependence of the phase boundaries.

In Fig. 1 the susceptibility and magnetization are shown as a function of external field at $T = 0.297$ K. The large peak in the susceptibility near 7 kOe is a result of the rapid increase in the magnetization at the AF-to-SF transition. The susceptibility attains a maximum value equal to $1/N$, within experimental uncertainty, where N is the demagnetizing factor ($4\pi/3$ for a sphere). In the SF state the susceptibility is almost constant and has a value slightly larger than the perpendicular susceptibility at small fields, as described in Sec. III. At the SF-to-P transition there is a small peak followed by a rapid drop in the susceptibility in the P state. The magnetization is calculated by numerical integration of the susceptibility. It shows the rapid increase at the AF-to-SF transition, followed by the increase within the SF state and saturation at the highest fields in the P state.

An expanded version of the susceptibility near the AF-to-SF transition is shown in the inset in Fig. 1. Typical error bars reflect an estimated 1.5% uncertainty in the absolute value of the susceptibility due to the calibration procedure outlined in Sec. III. The relative uncertainty between individual data points is an order of magnitude less than that shown by the error bars.

It has been shown by Levy[22] that the proper thermodynamic parameter for the description of the magnetic properties of an ellipsoidal sample is the shape-independent internal field

$$H_i = H_0 - NM \ , \tag{16}$$

where H_0 is the external field, N is the demagnetizing factor, and M is the magnetization of the sample. The susceptibilities obey the relation

$$\chi_i^{-1} = \chi_0^{-1} - N \ , \tag{17}$$

where $\chi_i = (\partial M/\partial H_i)_T$ and $\chi_0 = (\partial M/\partial H_0)_T$. At the AF-to-SF phase boundary the magnetization should be discontinuous in the internal field, and the differential susceptibility χ_i should be infinite. Experimentally, however, one measures χ_0, which from Eq. (17) has the value $1/N$ at the phase boundary. The measured value of χ_0 does equal $1/N$, within the limits of uncertainty shown in Fig. 1.

The susceptibility χ_i and the magnetization are plotted against the internal field in Fig. 2. Since χ_0 is consistent with the value $1/N$, the calculated maximum value of $\chi_i = 25.3$ emu/cm^3 is consistent with the expected value $\chi_i = \infty$ at a first-order transition. The increase in the magnetization takes place over a range of internal field of 10 Oe, which is just the calculated inhomogeneity in internal field expected from the known inhomogeneity of the superconducting solenoid and the experimental uncertainty in χ_0. The behavior of the susceptibility

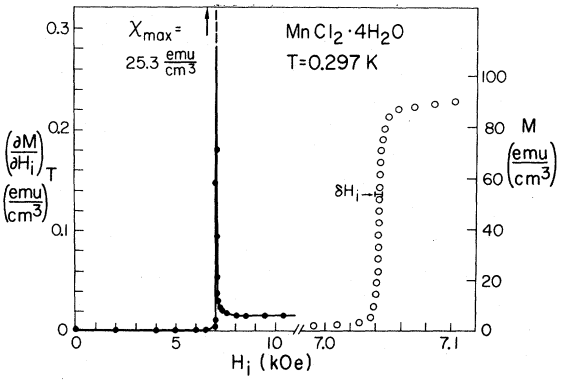

FIG. 2. Differential magnetic susceptibility and magnetization of $MnCl_2 \cdot 4H_2O$ as a function of internal field at 0.297 K with the external field along the preferred direction. ●, susceptibility (left-hand scale); o, magnetization (right-hand scale).

and magnetization in terms of the shape-independent internal field clearly establishes the first-order nature of the AF-to-SF transition in $MnCl_2 \cdot 4H_2O$ at a temperature of 0.297 K.

The susceptibility χ_0 as a function of external field in the neighborhood of the AF-to-SF transition at several different temperatures is shown in Fig. 3. At 0.372 K the behavior of χ_0 is basically the same as at 0.297 K, except that it does not quite attain the expected value of $1/N$ at the phase boundary. At higher temperatures the height of the susceptibility peak at the phase boundary decreases rapidly with increasing temperature.

The susceptibility χ_i and the magnetization as a function of internal field are plotted in Figs. 4 and 5. A definite change in behavior takes place between 0.372 and 0.426 K. At 0.372 K, although the maximum value of χ_i is somewhat smaller than at 0.297 K, the magnetization is discontinuous,

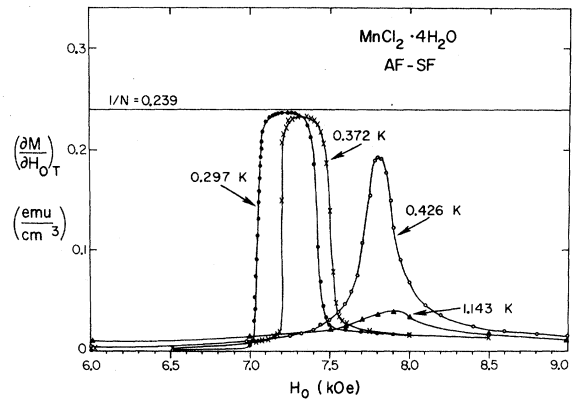

FIG. 3. Differential magnetic susceptibility of $MnCl_2 \cdot 4H_2O$ as a function of external field along the preferred direction near the AF-to-SF transition for several temperatures.

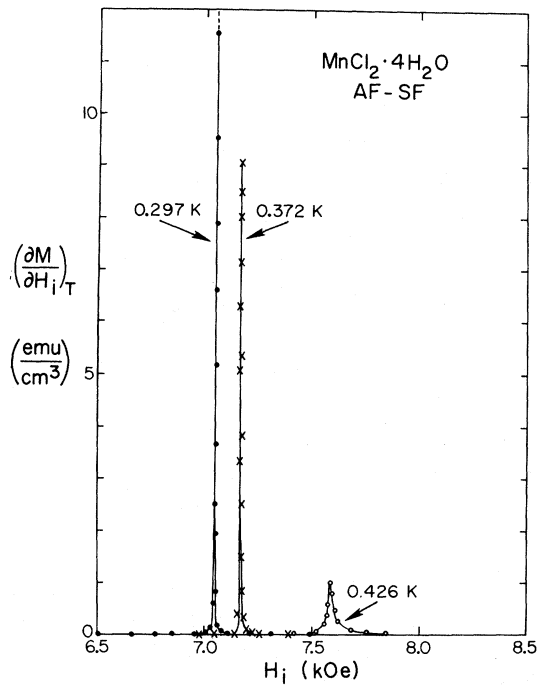

FIG. 4. Differential magnetic susceptibility of $MnCl_2 \cdot 4H_2O$ as a function of internal field near the AF-to-SF transition for several temperatures with the external field along the preferred direction.

within the uncertainty in H_i discussed above. However, at 0.426 K the magnetization no longer increases discontinuously. The first-order behavior has disappeared between 0.372 and 0.426 K. The susceptibility at 1.143 K has been left off in Fig. 4 since it reaches a maximum value of only 0.005 emu/cm^3 at the phase boundary.

The foregoing data provide substantial proof that the AF-to-SF transition in $MnCl_2 \cdot 4H_2O$ is first order at least up to 0.4 K. Since the alignment

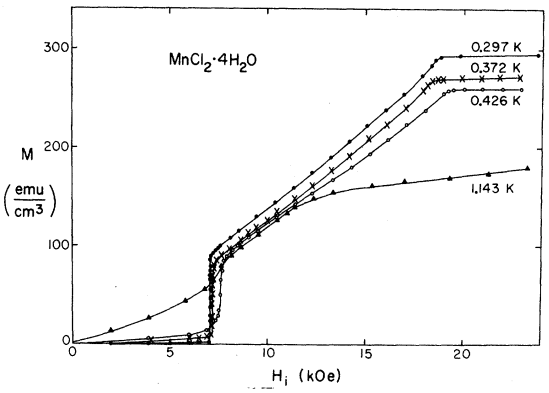

FIG. 5. Magnetization of $MnCl_2 \cdot 4H_2O$ as a function of internal field for several temperatures with the external field along the preferred direction.

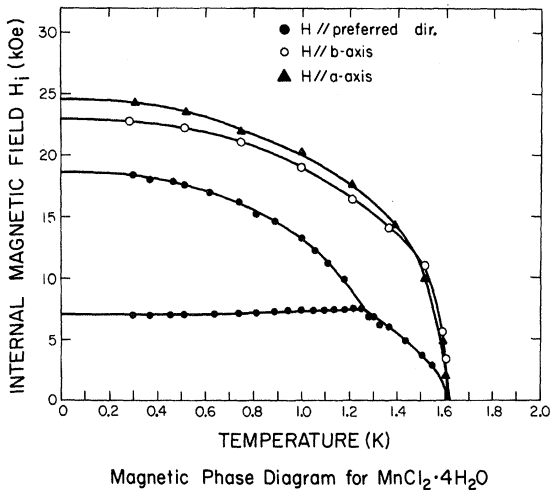

FIG. 6. H-T phase diagram for $MnCl_2 \cdot 4H_2O$ as determined from the differential magnetic susceptibility.

of the external field was known only to ± 2°, the disappearance of the first-order behavior above 0.4 K can be interpreted as evidence that the critical angle[12] ψ_c has decreased from its maximum value at $T = 0$ to ~ 2° at 0.4 K. From the experimentally calculated values of the effective exchange and anisotropy fields listed below, we estimate that $\psi_c = 6.5°$ at $T = 0$. If ψ decreases approximately linearly with increasing temperature then it goes to zero near 0.6 K. This implies that the first-order transition will not be observed above 0.6 K, and suggests that the bicritical point[23] may be as low as 0.6 K in this compound.

C. Temperature dependence of the phase boundaries

In addition to the data just presented, the susceptibility was measured at a series of temperatures in the neighborhood of the phase transitions in order to obtain the values of the critical internal fields as a function of temperature. The resulting H-T phase diagram is presented in Fig. 6. The solid circles are the data obtained with the external field along the preferred direction. The three phase boundaries separating the AF, SF, and P states are clearly indicated. With the external field along the a axis and b axis, respectively, there is only a single transition from the AF state to the P state at the critical internal fields indicated in Fig. 6. The behavior of the perpendicular susceptibility near the transition is similar to the behavior of the parallel susceptibility near the SF-to-P transition. The data for all the critical fields are tabulated in Table I.

The temperature dependence of the SF-to-P phase boundary is of particular importance, since according to Anderson and Callen[16] it should directly reflect the temperature dependence of the renormalized spin-wave energies. Based on their

TABLE I. Critical internal fields for $MnCl_2 \cdot 4H_2O$.

Magnetic field parallel to preferred direction					Magnetic field perpendicular to preferred direction		
T (K)	H_{c1} (kOe)	H_{c2} (kOe)	T (K)	H_c (kOe)	T (K)	H_{cb} (kOe)	H_{ca} (kOe)
0.00	7.065[a]	18.55[a]			0.00	22.95[a]	24.55[a]
0.297	7.040	18.390	1.281	6.884	0.287	22.760	
0.371	7.036	18.050	1.303	6.886	0.308		24.300
0.456	7.045		1.327	6.260	0.513	22.251	23.621
0.464		17.802	1.364	6.097	0.741		22.097
0.512	7.064	17.534	1.432	4.889	0.747	21.059	
0.617		17.039	1.507	3.749	1.002	19.034	20.229
0.637	7.123		1.548	2.892	1.207	16.508	17.697
0.738	7.174	16.181			1.390	13.847	14.349
0.811	7.211	15.234			1.515	11.035	10.040
0.891	7.324	14.569			1.591	5.542	4.906
0.943	7.352				1.605	3.352	2.121
1.002	7.391	13.163					
1.049	7.433						
1.056		12.198					
1.094	7.464						
1.110		11.200					
1.135	7.486						
1.179	7.500	9.921					
1.217	7.523						
1.248	7.529						

[a]Extrapolated values.

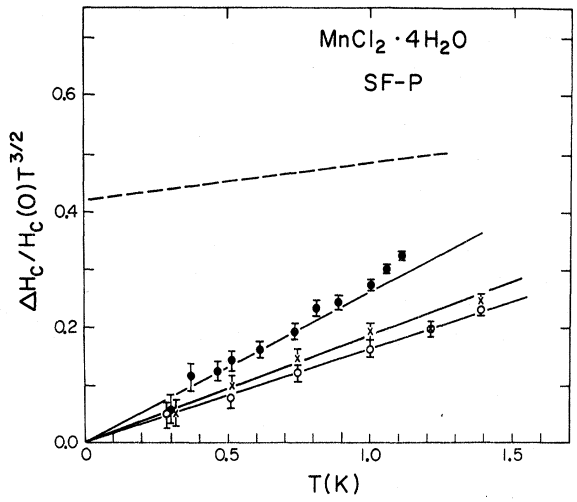

FIG. 7. Temperature dependence of phase boundaries bordering the paramagnetic phase at low temperatures for $MnCl_2 \cdot 4H_2O$. ●, H along the preferred direction; o, H along the b axis; ×, H along the a axis; dashed line, theory of Anderson and Callen (Ref. 16).

treatment of spin-wave interactions there should be a predominantly $T^{3/2}$ dependence. In order to compare the experimental data with the expected behavior given by Eq. (6), it is convenient to rewrite Eq. (6) in the form

$$\Delta H_{\parallel}^{c}(T)/H_{\parallel}^{c}(0)\,T^{3/2} \equiv [H_{\parallel}^{c}(0) - H_{\parallel}^{c}(T)]/H_{\parallel}^{c}(0)\,T^{3/2} = C_1 + C_2 T \,. \qquad (18)$$

Presented in this form the data are expected to produce a linear fit with intercept C_1 and slope C_2. However, the value of the critical field at $T = 0$, $H_{\parallel}^{c}(0)$, is unknown and must be determined in the analysis. It is treated as a parameter and is varied to obtain the best linear fit to the data when presented in the form of Eq. (18). The experimentally determined values of C_1 and C_2 are simply extracted from the resulting fit.

The data are shown in Fig. 7, where we present not only the data for the critical field for the SF-to-P transition (H parallel to the preferred direction), but also the critical fields for the two perpendicular directions. The solid lines represent the best fits to the data, and in all three cases a value of $C_1 = 0$ produced the best fit. The dashed line represents the behavior expected from the theory of Anderson and Callen[16] as applied to the case of $MnCl_2 \cdot 4H_2O$, for which the values of the constants C_1 and C_2 are calculated to be 0.42 and 0.064, respectively. Since C_1 is found to be zero, there is no experimental evidence for a $T^{3/2}$ dependence for the critical fields bordering the paramagnetic state in $MnCl_2 \cdot 4H_2O$. This is inconsistent with the Anderson-Callen model for a simple cubic antiferromagnet.

The data at the highest temperatures for H along the preferred direction deviate significantly from the linear form of Eq. (18), suggesting the presence of a higher-order temperature dependence. Assuming C_1 is exactly zero from the above analysis, both sides of Eq. (18) can be divided by T. Any higher-order terms will cause the data to deviate from a horizontal straight line of magnitude C_2 when $\Delta H^c(T)/H^c(0)\,T^{5/2}$ is plotted against temperature. The results are shown in Fig. 8. It is seen that the data for H along the preferred direction are consistent with an additional $T^{7/2}$ term which is significantly greater than zero. The solid lines again represent the best fits to the data. In the two perpendicular directions the data are not entirely inconsistent with the absence of a higher-order contribution, although the best fit has a small positive slope. The values of the critical fields, extrapolated to $T = 0$, found from the above analysis are

for H parallel to the preferred direction,

$$H_{\parallel}^{c}(0) = 18.55 \pm 0.05 \text{ kOe};$$

for H parallel to the b axis,

$$H_{\perp 1}^{c}(0) = 22.95 \pm 0.05 \text{ kOe};$$

and for H parallel to the a axis,

$$H_{\perp 2}^{c}(0) = 24.55 \pm 0.05 \text{ kOe}.$$

The experimentally determined coefficients C_1, C_2, and C_3 are tabulated in Table II, along with the values of C_1 and C_2 calculated from the theory of Anderson and Callen[16] and the value of C_1 calculated from the theory of Feder and Pytte.[18]

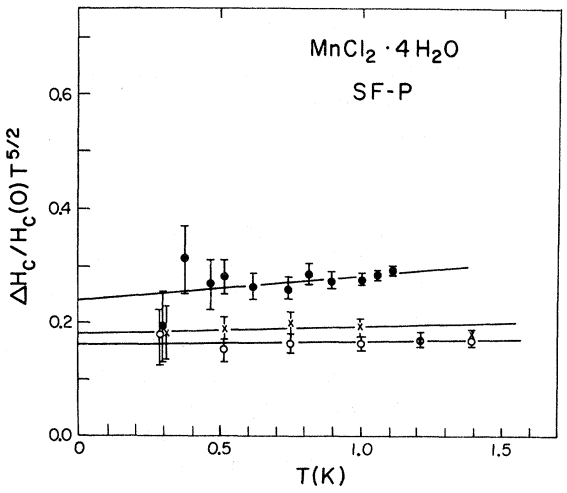

FIG. 8. Temperature dependence of phase boundaries bordering the paramagnetic phase at low temperatures for $MnCl_2 \cdot 4H_2O$. ●, H along the preferred direction; o, H along the b axis; ×, H along the a axis.

TABLE II. Comparison of theoretical and experimental critical-field parameters for $H^c = H^c(0)\,(1 - C_1 T^{3/2} - C_2 T^{5/2} - C_3 T^{7/2})$. SF-to-P transition and perpendicular AF-to-P transitions in $MnCl_2 \cdot 4H_2O$.

	C_1	C_2	C_3
Theory			
AC (Ref. 16)	0.42	0.064	...
FP (Ref. 18)	0.42	...	...
Experimental			
preferred direction	0.00 ± 0.02	0.240 ± 0.02	0.04 ± 0.01
b axis	0.00 ± 0.015	0.160 ± 0.015	0.008 ± 0.004
a axis	0.00 ± 0.015	0.180 ± 0.01	0.010 ± 0.008

The expected temperature dependence of the AF-to-SF phase boundary is given by Eq. (5) for both uniaxial single-ion anisotropy and anisotropic exchange. Again, it is convenient to express Eq. (5) in the form

$$\Delta H_{\parallel}^{sf}(T)/H_{\parallel}^{sf}(0)\,T^{3/2} \equiv [H_{\parallel}^{sf}(T) - H_{\parallel}^{sf}(0)]/H_{\parallel}^{sf}(0)\,T^{3/2} = -A + B\,T^{5/2}. \quad (19)$$

In this case only the lowest-temperature data are included in the analysis, since Eq. (5) is valid only for $T \ll T_{AE} = g\mu_B H_{\parallel}^{sf}(0)/k_B \simeq 1.0$ K. The data are shown in Fig. 9, where the solid line represents the best fit to the data, and the dashed line is the expected behavior for single-ion anisotropy for the case of $MnCl_2 \cdot 4H_2O$. The presence of a nonzero value for the coefficient A strongly suggests that single-ion anisotropy is dominant in this compound. From the analysis of the data, we obtain

$$\Delta H_{\parallel}^{sf}(0) = 7.065 \pm 0.01 \text{ kOe},$$
$$A = 0.066 \pm 0.007 \text{ K}^{-3/2},$$
$$B = 0.129 \pm 0.020 \text{ K}^{-5/2}.$$

The calculated values of A and B from Feder and Pytte[18] for $MnCl_2 \cdot 4H_2O$ are

$$A_{calc} = 0.066 \text{ K}^{-3/2},$$
$$B_{calc} = 0.177 \text{ K}^{-5/2}.$$

Using the experimentally determined values of A and B, we find that the data are consistent with the existence of a minimum in the phase boundary at $T_{min} = 0.6A/B = 0.307$ K.

At temperatures above the bicritical point there is a second-order transition from the AF state to the P state with the external field along the preferred direction. This transition has been investigated previously by Gijsman, Poulis, and Van den Handel[7] using NMR and electron-resonance techniques, and by Reichert, Butera, and Schiller[5] with specific-heat and magnetization measurements. However, both of these investigations were performed with the external field along the *c* axis and, therefore, give a phase boundary slightly different from the true phase boundary with the field along the preferred direction.

In the present experiment the differential susceptibility as a function of magnetic field exhibits a single rather broad peak at all temperatures between the bicritical point and T_N. The field value corresponding to the maximum in the susceptibility is chosen as the critical field. The data are shown in Fig. 10 as a function of temperature. The solid circles are the present results, while the open circles and the crosses are the results of Reichert *et al.*[5] and Gijsman *et al.*,[7] respectively. The critical fields in the present case are substantially lower at all temperatures than the earlier results along the *c* axis.

The temperature dependence of the AF-to-P phase boundary has been treated by a number of authors in the limit $H = 0$. Besides the mean-field model[14] which predicts a quadratic dependence of $T_N(H)$ on magnetic field, i.e., $T_N(H)/T_N(0) \sim 1 - \gamma H^2$, the only known calculations of the phase boundary in finite fields are the Ising-model calculations of Fisher[24] and Bienenstock,[25] and more recently the Monte Carlo calculations on Ising systems by Landau.[26] The two-dimensional superexchange model considered by Fisher leads to a quadratic dependence of T_N on H in the limit $H = 0$. The work of Bienenstock can be expressed by the relation $T_N(H) = T_N(0)[1 - (H/H_c)^2]^{\zeta}$, where $\zeta = 0.87$, 0.35, and 0.36 for the square, sc, and bcc lattices, respectively. This reduces to a quadratic dependence

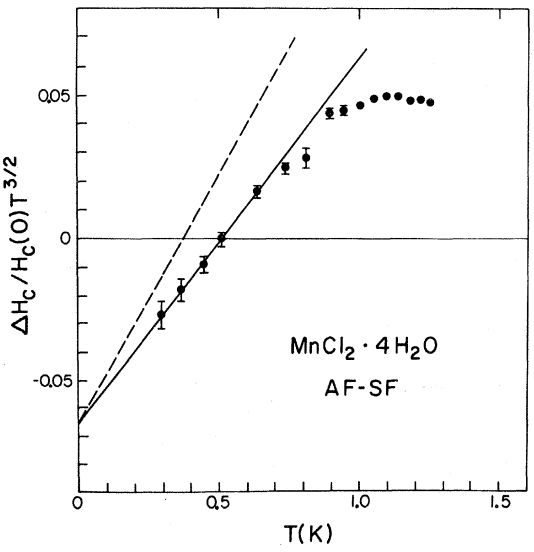

FIG. 9. Temperature dependence of the AF-to-SF phase boundary for $MnCl_2 \cdot 4H_2O$. ●, data; solid line, best fit to the data for $T \lesssim 0.6$ K; dashed line, theory of Feder and Pytte (Ref. 18).

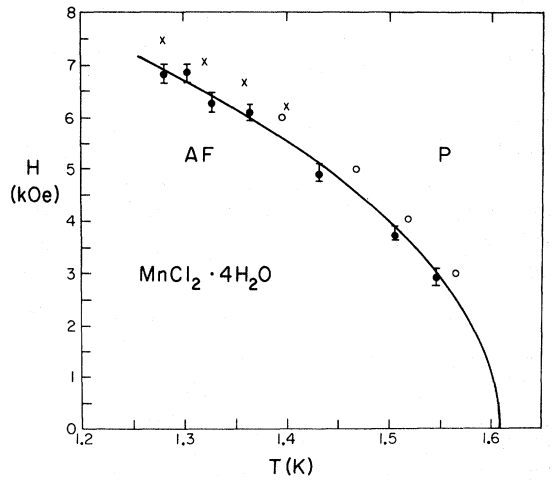

FIG. 10. Temperature dependence of the AF-to-P phase boundary for $MnCl_2 \cdot 4H_2O$. ●, present data; solid line, best fit to present data; o, data of Reichert, Butera, and Schiller (Ref. 5); +, data of Gijsman, Poulis, and Van den Handel (Ref. 7).

in the limit $H=0$. However, for the three-dimensional lattices at larger fields the variation of T_N with field is considerably slower than quadratic. Landau has shown that the value of ζ is not completely determined by dimensionality and that, in fact, it can take on a range of values which depend on the details of the interactions considered.

In any event, it is not clear that any of the Ising-model calculations should be expected to reproduce the phase boundary in $MnCl_2 \cdot 4H_2O$. Many of the features of this compound appear to be well represented by the anisotropic Heisenberg model. On the other hand, Fisher and Sykes[27] found that the zero-field susceptibility of $MnCl_2 \cdot 4H_2O$ is surprisingly similar to the susceptibility of the bcc Ising system.

Experimentally we find the data can be described very well, over the entire temperature range, by a quadratic relation of the form $T_N(H)/T_N(0) = 1 - \gamma H^2$, with $\gamma = 4.3 \times 10^{-9}$ Oe^{-2}. This is shown by the solid curve in Fig. 10. Previously it has been found that the antiferromagnetic compounds $CoCl_2 \cdot 6H_2O$ (Ref. 28) and $MnBr_2 \cdot 4H_2O$ (Ref. 29) are also consistent with this simple form over the entire temperature range.

The temperature dependence of the phase boundaries very close to the bicritical point is of particular importance in view of the recent discussions of Fisher and Nelson.[23] Unfortunately, the present data do not allow us to draw any conclusions about this very important point.

D. Exchange and anisotropy energies

The two perpendicular directions are found to be nonequivalent in $MnCl_2 \cdot 4H_2O$. It is expected, therefore, that the biaxial anisotropy model should be appropriate in this case. Equations (2), (3), (10), and (11) give the critical fields at $T=0$ in terms of the effective exchange and anisotropy fields. Possible anisotropic exchange contributions are expected to be small and will be discussed later. In Eqs. (2) and (3), h_A should be replaced by h_{A1} for the biaxial model. Inserting the experimentally determined values for the critical fields bordering the paramagnetic state in Eqs. (3), (10), and (11) we obtain

$$h_E = 10.375 \pm 0.03 \text{ kOe},$$

$$h_{A1} = 2.20 \pm 0.05 \text{ kOe},$$

and

$$h_{A2} = 3.80 \pm 0.05 \text{ kOe}.$$

It was not necessary to use Eq. (2) to determine the effective fields. However, it may be used as a self-consistency test of the model. Inserting the above values of h_E and h_{A1} in Eq. (2) we calculate $H_{\parallel}^{sf}(0) = 7.10$ kOe, which is within the calculated limits of uncertainty of the experimentally determined value of 7.065 ± 0.05 kOe.

The observed temperature dependence of the AF-to-SF transition suggested that single-ion anisotropy dominates any possible anisotropic exchange in $MnCl_2 \cdot 4H_2O$. We can place an upper limit on the effective anisotropic exchange field h_{AK} by including it in the critical-field expressions. From spin-wave and mean-field theory we get

$$H_{\parallel}^{c}(0) = 2h_E + h_{AK} - h_{A1} \tag{20}$$

and

$$H_{\perp 1}^{c}(0) = 2h_E + h_{AK} + h_{A1}. \tag{21}$$

From mean-field theory the upper limit of stability of the AF state, which does not differ significantly from the true thermodynamic transition in $MnCl_2 \cdot 4H_2O$, can be written

$$H_{\parallel}^{sf}(0) = [(2h_E + h_{AK} + h_{A1})(h_{AK} + h_{A1})]^{1/2}. \tag{22}$$

Inserting the data in Eqs. (20)–(22) we find

$$h_{AK} = 0.00 \pm 0.025 \text{ kOe},$$

with h_E and h_{A1} the same as above.

E. AF-to-SF transition and first order

The observed temperature dependence of the AF-to-SF phase boundary was found to be consistent with the spin-wave theory of Feder and Pytte,[18] which predicts a minimum in the phase boundary for uniaxial anisotropy. A linear plot of the experimental data is shown in Fig. 11, where the solid line is the best fit to the data up to 0.6 K as indicated above in Fig. 11. The shallow minimum

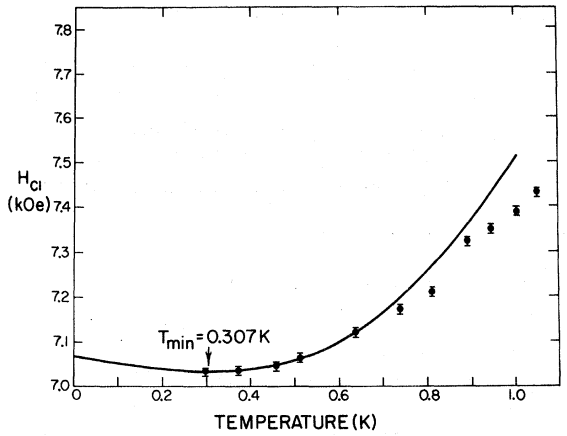

FIG. 11. Low-temperature portion of the AF-to-SF phase boundary for $MnCl_2 \cdot 4H_2O$. ●, data; solid line, best fit to data from theory of Feder and Pytte (Ref. 18).

at $T_{min} = 0.307$ K is clearly evident. The lack of data below 0.297 K means that the values of the parameters derived from the fit should be viewed with some skepticism; however, the existence of the minimum appears well established. For a first-order phase transition the latent heat is related to the slope of the phase boundary by the Clausius-Clapeyron equation, which for magnetic systems can be written in the form

$$l = T\Delta M\left(\frac{dH_c}{dT}\right), \tag{23}$$

where l is the latent heat and ΔM is the increase in the magnetization in going from the AF to the SF state. At T_{min}, then, the latent heat must vanish. The vanishing of the latent heat at T_{min} also implies a lack of hysteresis accompanying the first-order transition. Hysteresis at the AF-to-SF transition as a function of internal field has not been previously observed, a fact which generally has been attributed to impurity or imperfection nucleation. However, it is quite possible that the true first-order transition was absent in these cases due to misalignment.

In the present work no evidence of hysteresis was found at $T = 0.297$ K, which is not significantly different from T_{min}. However, at $T = 0.372$ K a "superheating" effect was observed during one experimental run. The value of the external field at which the transition was initiated exceeded by 150 Oe the initiation field that was observed during two "normal" runs. The complete absence of hysteresis at 0.297 K and the superheating that was observed at 0.372 K are consistent with a first-order transition with a minimum in the phase boundary at 0.3 K.

V. DISCUSSION AND CONCLUSIONS

From the measurement of the differential magnetic susceptibility, we have been able to observe the various magnetic phase transitions which occur in $MnCl_2 \cdot 4H_2O$. The AF-to-SF transition was studied in some detail. We observed first-order behavior up to $T \simeq 0.4$ K. The primary argument in support of this conclusion concerns the behavior of χ_0, which reaches a value of $1/N$ at the phase boundary, within experimental uncertainties, and remains at this value over a range of about 300 Oe in H_0. The internal field H_i, obtained by applying proper demagnetizing corrections to H_0, remains constant over this range in H_0. At this constant value of H_i the susceptibility χ_i is infinite and the magnetization increases discontinuously.

It is important to mention again that the first-order transition will be observed only if the external field, as shown by Rohrer and Thomas,[12] is within a small critical angle with respect to the magnetically preferred direction. Outside this critical angle the moments will rotate rapidly, but continuously, from the antiparallel alignment to the essentially perpendicular alignment of the spin-flop state. According to Blazey *et al.*[13] the critical angle will decrease with increasing temperature, going to zero at the bicritical point where the three phase boundaries meet. The present results are somewhat puzzling on this point. From Fig. 6 the phase boundaries appear to meet at 1.25 K. From the loss of the first-order behavior of the AF-to-SF transition it appears that the bicritical point might be considerably lower, $\simeq 0.6$ K. However, it is quite likely that the critical angle does not extrapolate to zero as rapidly as proposed. Thus, the bicritical point is most probably close to 1.25 K.

The temperature dependence of the phase boundaries was also determined and compared with spin-wave theory.[16,18] Anderson and Callen[16] include spin-wave interactions to determine the renormalized spin-wave energies. For cubic symmetry they show that the temperature dependence of the SF-to-P phase boundary should exactly reflect the temperature dependence of the renormalized spin-wave energies, which they find to have a predominantly $T^{3/2}$ dependence. Feder and Pytte[18] obtain an identical result in their work. Experimentally we find in $MnCl_2 \cdot 4H_2O$ that there is no evidence of a $T^{3/2}$ term in the temperature dependence. The dominant term is $T^{5/2}$ with evidence of higher-order contributions.

At the present time the nature of the discrepancy is unknown. As the phase boundary is approached from the P state the paramagnetic mode goes soft at the zone corner.[16] However, in the SF phase the low-energy SF mode continuously changes from

a linear function of wave vector, near $k=0$, to a quadratic function of k as the SF-to-P phase boundary is approached. It has been suggested that to describe properly this situation, the spin-wave interactions might have to be treated to higher order than the first-order treatments of Anderson and Callen[16] and Feder and Pytte.[18]

ACKNOWLEDGMENTS

It is with great pleasure that we acknowledge the many helpful discussions with D. P. Landau and M. H. Lee. We also wish to thank H. B. Callen and R. S. Silberglitt for their kind assistance in the interpretation of many of these results.

---

†Research supported in part by the National Science Foundation Grant No. GH-32228.

*Present address: 200 Seven Oaks Road, Durham, N.C.

[1]John E. Rives, Phys. Rev. 162, 491 (1967).

[2]W. F. Giauque, R. A. Fisher, E. W. Hornung, and G. E. Brodale, J. Chem. Phys. 52, 2901 (1970); 52, 3936 (1970); 53, 1474 (1970).

[3]T. A. Reichert and W. F. Giauque, J. Chem. Phys. 50, 4205 (1969).

[4]J. N. McElearney, H. Forstat, and P. T. Bailey, Phys. Rev. 181, 887 (1969).

[5]T. A. Reichert, R. A. Butera, and E. J. Schiller, Phys. Rev. B 1, 4446 (1970).

[6]M. Abkowitz and A. Honig, Phys. Rev. 136, A1003 (1964).

[7]H. M. Gijsman, N. J. Poulis, and J. Van den Handel, Physica 25, 954 (1959).

[8]A. Zalkin, J. D. Forrester, and D. H. Templeton, Inorg. Chem. 3, 529 (1963).

[9]Z. M. El Saffar and G. M. Brown, Acta. Crystallogr. B 27, 66 (1971).

[10]R. D. Spence and V. Nagarajan, Phys. Rev. 149, 191 (1966).

[11]R. F. Altman, S. Spooner, J. E. Rives, and D. P. Landau, Phys. Rev. B 11, 458 (1975).

[12]H. Rohrer and H. Thomas, J. Appl. Phys. 40, 1025 (1969).

[13]K. W. Blazey, H. Rohrer, and R. Webster, Phys. Rev. B 4, 2287 (1971).

[14]T. Magamiya, K. Yosida, and R. Kubo, Adv. Phys. 4, 1 (1955).

[15]C. J. Gorter and T. Van Peski-Tinbergen, Physica 22, 273 (1956).

[16]F. B. Anderson and H. B. Callen, Phys. Rev. 136, A1068 (1964).

[17]F. J. Dyson, Phys. Rev. 102, 1217 (1956); 102, 1230 (1956).

[18]J. Feder and E. Pytte, Phys. Rev. 168, 640 (1968).

[19]Y. L. Wang and H. B. Callen, J. Phys. Chem. Solids 25, 1459 (1964).

[20]F. Keffer, in *Handbuch der Physik*, edited by S. Flügge (Springer-Verlag, New York, 1966), Vol. 18/2, p. 108.

[21]J. E. Rives, in *Transition Metal Chemistry*, edited by R. L. Carlin (Dekker, New York, 1972), Vol. 7, pp. 1–86.

[22]P. M. Levy, Phys. Rev. 170, 595 (1968).

[23]The point of intersection of the three phase boundaries has recently been shown to be a unique type of critical point called a bicritical point. See for instance, M. E. Fisher and D. R. Nelson, Phys. Rev. Lett. 32, 1350 (1974).

[24]M. E. Fisher, Proc. R. Soc. A 254, 66 (1960); 256, 502 (1960).

[25]A. Bienenstock, J. Appl. Phys. 37, 1459 (1966).

[26]D. P. Landau, Bull. Am. Phys. Soc. Ser. II 15, 1380 (1970), and unpublished.

[27]M. E. Fisher and M. F. Sykes, Physica 28, 939 (1962).

[28]J. Skalyo, Jr., A. F. Cohen, S. A. Friedberg, and R. B. Griffiths, Phys. Rev. 164, 705 (1967).

[29]J. H. Schelleng and S. A. Friedberg, Phys. Rev. 185, 728 (1969).